Research Article *ISSN: 2319-507X*
Nishanth P, IJPRET, 2013; Volume 1(8): 11-22 *IJPRET*

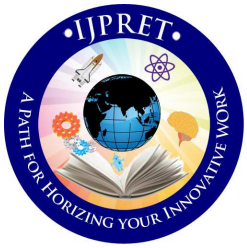

INTERNATIONAL JOURNAL OF PURE AND APPLIED RESEARCH IN ENGINEERING AND TECHNOLOGY

A PATH FOR HORIZING YOUR INNOVATIVE WORK

MODELING AND FLOW ANALYSIS OF MODERN FIGHTER AIRCRAFT CONFIGURATION USING -CFD

IJPRET-QR CODE

NISHANTH.P[1], N.RAJAMURUGU[2],

ABILDEV.P[3]

PAPER-QR CODE

1. **Assistant Professor, Department of Aeronautical Engineering, MVJCE, Bangalore.**
2. **Assistant Professor, Department of Aeronautical Engineering, MVJCE, Bangalore.**
3. **UG student, Project Assistant, Department of Aeronautical Engineering, MVJCE, Bangalore.**

Accepted Date:

03/03/2013

Publish Date:

01/04/2013

Keywords

Canard,

Downwash Effects,

CFD

Corresponding Author

Mr. Nishanth. P

Abstract

The use of canard in advanced aircraft for control and improved aerodynamic performance is a topic of continued interest and research. The canard is a control device, which is placed in front of main wing adding to increase in maximum lift and decrease in drag. The presence of canard in close proximity to the wing results in a highly coupled canard-wing aerodynamic flow field which can include downwash/upwash effects, vortex-vortex interactions and vortex-surface interactions. Emphasis is placed on the effects of canard on aerodynamic performance and further comparison is made with and without canard configuration.

1. INTRODUCTION

A primary purpose of fighter aircraft is to destroy other aircraft, either in offensive or defensive modes of operation, or to pose such a compelling threat that enemy air operations are effectively curtailed. Enemy fighters, bombers, patrol and reconnaissance aircraft, as well as ground-support and transport aircraft, are the prey of the fighter. To perform its intended function, the fighter must be able to reach a favorable position for inflicting crippling damage on the enemy. This means that the fighter pilot must first be able to detect the enemy aircraft; the methods of detection employed in the First World War were primarily visual. Thus, the aircraft and pilot's position in it must be designed to provide the widest possible field of view. Detection means little, however, unless the aircraft possesses the performance and maneuverability necessary to achieve a favorable attack position and provides a steady gun platform together with sufficiently powerful armament to destroy the enemy once a favorable position has been achieved. Some of the performance and maneuverability characteristics of importance are speed in various flight conditions, rate of climb and ceiling, roll rate, turning radius and climb capability while in a turn, and range and endurance.

The “tailless delta-canard” configuration has the horizontal control surfaces moved forward to become a canard in front of the wing. When the aircraft pitches up, instead of forcing the tail down decreasing overall lift, the canard lifts the nose, increasing the overall lift. Because the canard is picking up the fresh air stream instead of the wake behind the main wing, the aircraft can achieve better control authority with a smaller-size control surface, thus resulting in less drag and less weight.

Canard Aircraft Characteristics

Canard foreplanes act in a similar way to conventional tailplane and elevators, but due to swap in position about the centre of gravity control surface actions have the opposite effect.

A canard arrangement produces more lift than a conventional set-up when total lift produced is considered. During manoeuvres the canard control surfaces mirror those of

the main wing, adding to the lift to climb and decreasing the lift to descend. This means that the aircraft can move tighter and faster than with a conventional set-up.

The wing root operates in the downwash from the canard surface, which reduces its efficiency, although the effect of the downwash does not cause as large of a problem as the tailplane would experience in a conventional set-up.

The wing tips operate in the upwash from the canard surface, which increases the angle of attack on the tips and promotes premature separation of the air flowing over the wing tip. This premature separation at one tip or the other would promote wing-drop at the approach to the stall, leading to a spin. This must be avoided by precautions in the design of the wing, and may require extra weight in the wing structure outboard of the wing root.

Because the canard must be designed to stall before the main wing, the main wing never stalls and so never achieves its maximum lift coefficient. This may require a larger wing to provide extra wing area in order for the airplane to achieve the desired takeoff and landing distance performance.

2. PROBLEM STATEMENT AND ANALYSIS

The major objective of the present project is to compute the aerodynamic forces and moment coefficient through CFD package HYENA for a typical modern fighter canard controlled aircraft configuration for the following cases:

i) Canard deflection at δ_c = 0 deg; with variation in angle of attack

ii)Canard deflection at δ_c = +10 deg; with variation in angle of attack

iii)Canard deflection at δ_c = -10 deg; with variation in angle of attack

The scope of the present work is detailed as follows;

Geometric modelling of the typical candidate canard controlled fighter aircraft configuration using CATIA V5 modeling software. Smoothening of the individual components of the modern fighter aircraft using CATIA V5 .Meshing of the aircraft using ANSYS ICEMCFD.Analysis through

HYENA CFD code,Studying the streamline using TECPLOT360 Studying the pressure contour using TECPLOT360.

This analysis was carried out on the principle of control volume method, where the aircraft is fixed in space with the fluid moving through it.

The analysis has been carried out for various canard deflection angles such as -10deg, 0deg, +10deg. For each canard deflection angles various angle of attack conditions have been implemented such as 2.5^0, 5^0, 7.5^0, 10^0, 12.5^0, and 15^0. The pitching moment reference point is located ahead of c.g. i.e. at the nose of the aircraft

Further, CFD analysis has been carried out for the same aircraft without canard and the results have been compared with the aircraft having canard.

3. CFD Analysis Results

The fighter aircraft with canard is considered as candidate geometry for the present analysis. The analysis has been carried out considering the principle that if canard is present the total lift of the aircraft will be increased. Keeping this principle various canard deflection angles and various angle of attack was implemented for the aircraft configuration, similarly the analysis was also carried for aircraft without canard. The flow conditions are taken same for all the configurations. The flow conditions have been listed in table 3.1

3.2.1 CASE 1:Predicted CFD results for canard deflection angle 0deg with variation in Angle of Attack

CFD predictions have been carried out for the fighter aircraft with 0deg canard deflection angle. The streamlines pattern and pressure coefficient contour for different angle of attack conditions are shown from the figure 3.2 to3.7. The generated grid cell was 16lakhs. The coefficient of lift, coefficient of drag and coefficient of pitching moment are the outputs from the HYENA analysis software. The graphs plotted shown in the fig 3.8 to 3.10.

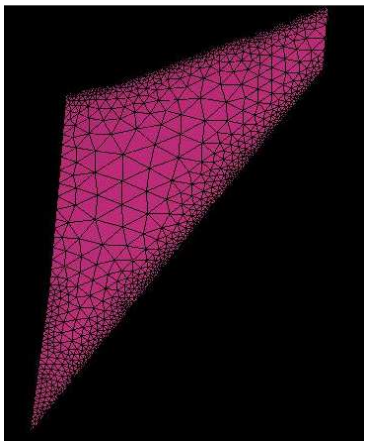

Fig 3.1 Generation of Tetrahedral mesh for canard surface

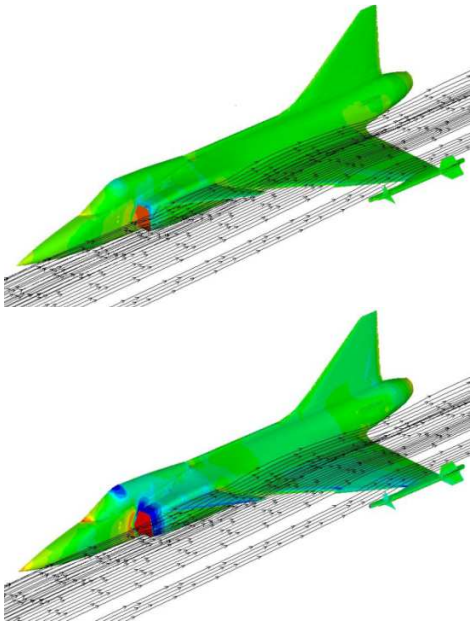

Fig 3.2 Streamline and Pressure contour for α=2.5deg; δ_c = 0deg, M=0.5

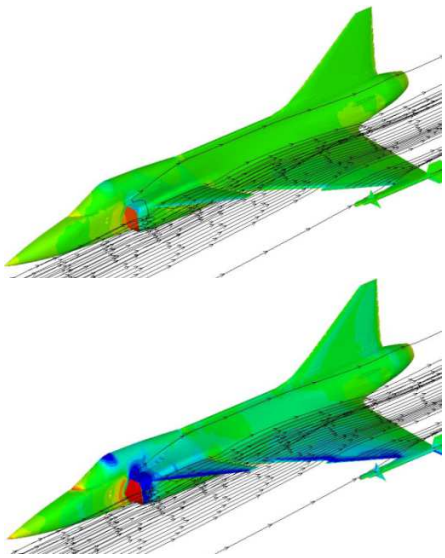

Fig 3.3 Streamline and Pressure contour for α=5deg; δ_c = 0deg, M=0.

3.2.2 CASE 2 Predicted CFD results for canard deflection angle +10deg with variation in Angle of Attack

The canard is deflected to an angle of 10deg and the coefficient of drag, coefficient of lift, and coefficient of pitching moment values has been obtained at this position of canard. The difference between case1 and case2 is change in the canard deflection angle. It is clear from the graph that the coefficient of lift increases with increase in canard angle. The generated grid cell was 18lakhs. The streamline and pressure coefficient contours are shown in the fig

3.11 to 3.16. The graphs are plotted shown in the fig 3.17 to 3.19.

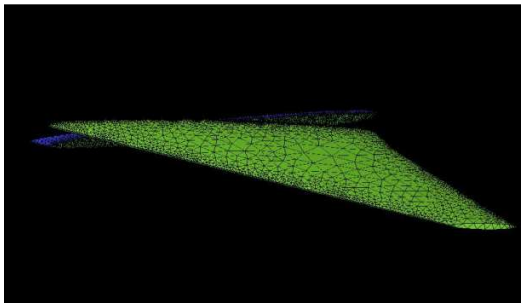

Fig 3.11 Generation of Tetrahedral mesh for canard surface with 10deg deflection

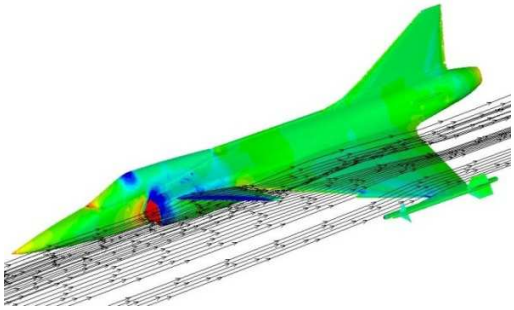

Fig 3.12 Streamline and Pressure contour for α=2.5deg; δ_c = 10deg, M=0.5

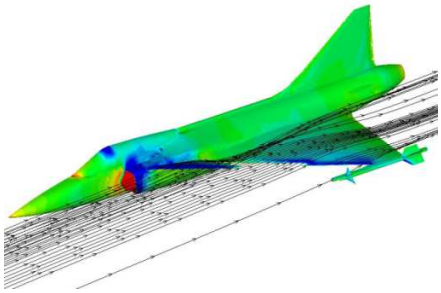

Fig 3.13 Streamline and Pressure contour for α=5deg; δ_c = 10deg, M=0.5

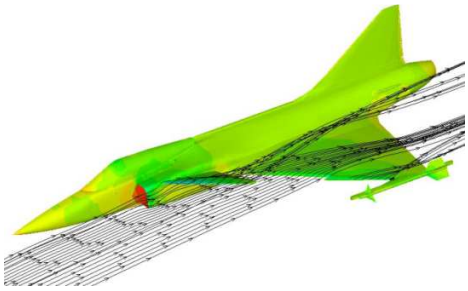

Fig 3.14 Streamline and Pressure contour for α=7.5deg; δ_c = 10deg, M=0.5

Angle of Attack (deg)	Coefficient of Lift (C_L)	Coefficient of Drag (C_D)	Coefficient of Pitching Moment (C_M)
2.5	8.19E-02	-1.04E-02	1.19E-01
5	1.85E-01	3.11E-03	2.89E-01
7.5	2.87E-01	2.54E-02	4.55E-01
10	3.88E-01	5.66E-02	6.22E-01
12.5	4.89E-01	9.74E-02	7.94E-01
15	5.87E-01	1.47E-01	9.67E-01

Tab 8.2 Computed results of C_L, C_D, C_m for δ_c = +10deg with variation in Angle of attack

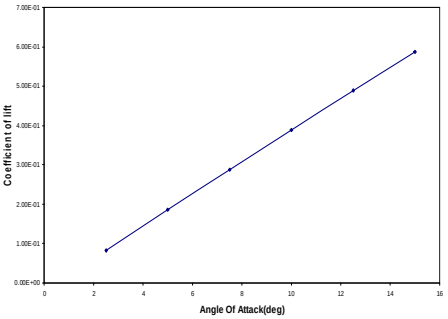

Fig 3.18 Coefficient of lift V_s Angle Of Attack for 10deg canard deflection angle

3.2.3 CASE 3 Predicted CFD results for canard deflection angle

-10deg with variation in Angle of Attack

The canard is deflected to an angle of -10deg and the coefficient of drag, coefficient of lift and coefficient of pitching moment values has been obtained at this position of canard. The difference between case2 and case3 is change in the canard deflection angle to negative. The generated grid cell was 18lakhs. The streamline and pressure coefficient contours are shown in the fig 3.20 to 3.25. The graphs are plotted shown in the fig 3.26 to 3.28.

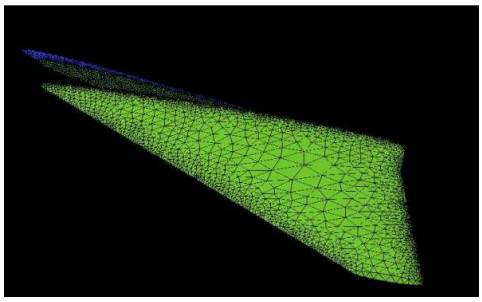

Fig 3.21 Generation of Tetrahedral mesh for canard surface with -10deg deflection

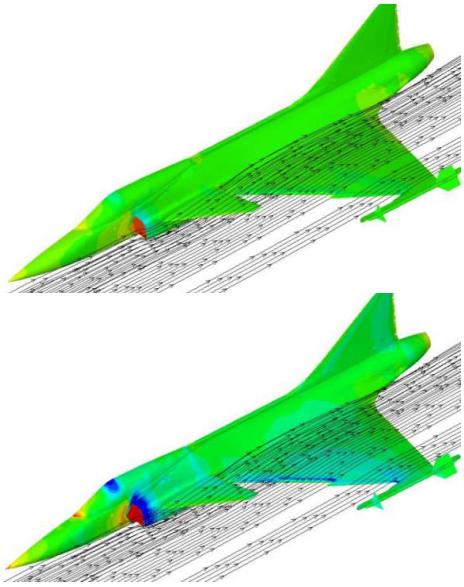

Fig 3.22 Streamline and Pressure contour for α=2.5 deg; δ_c = -10deg, M=0.5

Angle of Attack (deg)	Coefficient of Lift (C_L)	Coefficient of Drag (C_D)	Coefficient of Pitching Moment (C_M)
2.5	6.92E-02	-8.27E-03	1.20E-01
5	1.70E-01	7.88E-03	2.85E-01
7.5	2.70E-01	3.36E-02	4.50E-01
10	3.66E-01	6.78E-02	6.14E-01
12.5	4.63E-01	1.10E-01	7.83E-01
15	5.62E-01	1.61E-01	9.60E-01

Tab 8.3 Computed results of C_L, C_D, C_m for δ_c = -10deg with variation in Angle of attack

3.2.4 CASE 4: Predicted CFD results for no canard configuration with variation in Angle of Attack

In the above three cases in which we considered canard and different deflection for canard, where as in this case CFD prediction have been carried for the same fighter aircraft configuration with the absences of canard. From the above three cases we have seen variation in the coefficient of lift and coefficient of drag, when subjected to different canard deflection angles and with different angle of attack (AOA) conditions. In the above three cases the coefficient of lift increases with decrease in coefficient of drag. The streamline and pressure coefficient contour for different angle of attack conditions are shown in the figure 3.29 to 3.34. The generated grid cell was 16lakhs. The graphs are plotted shown in the fig 3.35 to 3.37.

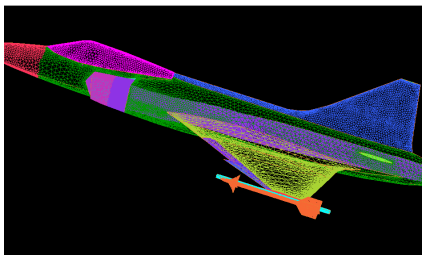

Fig 3.31 Generation of Tetrahedral mesh for the complete aircraft without canard configuration

Angle of Attack (deg)	Coefficient of Lift (C_L)	Coefficient of Drag (C_D)	Coefficient of Pitching Moment (C_M)
2.5	7.20E-02	-7.49E-03	**1.22E-01**
5	1.68E-01	7.29E-03	**2.85E-01**
7.5	2.57E-01	3.03E-02	**4.40E-01**
10	3.42E-01	5.97E-02	**5.87E-01**
12.5	4.29E-01	9.54E-02	**7.45E-01**
15	**5.21E-01**	**1.42E-01**	**9.15E-01**

Tab 8.4 Computed results of C_L, C_D, C_m for No Canard configuration with variation in Angle of attack

3.2.5 CASE 5: Comparison of Predicted CFD Results With And Without Canard Configuration

In fighter aircraft coefficient of lift is mattered more, this case is carried out to check the effectiveness of canard, from the graph 3.41 to 3.46 it is evident that the presence of canard gives more coefficient of lift then the aircraft without canard configuration.

From Fig 3.41 and 3.42, here the canard deflection angle is kept at 0deg and compared with that of no canard. From the graph plotted the coefficient of lift increases then that of without canard configuration where as the coefficient of drag remains constant with that of no canard configuration.

From Fig 3.43 and 3.44, here the canard deflection angle +10deg are compared with no canard configuration. From the graph plotted we can see increase in coefficient of lift for canard configuration with 10deg deflection, where as the coefficient of drag decreases and remains constant, this condition proves that the presences of canard comparatively increases coefficient of lift and decrease in coefficient of drag.

From Fig 3.45 and 3.46, here the canard deflection angle -10deg is compared with without canard configuration.

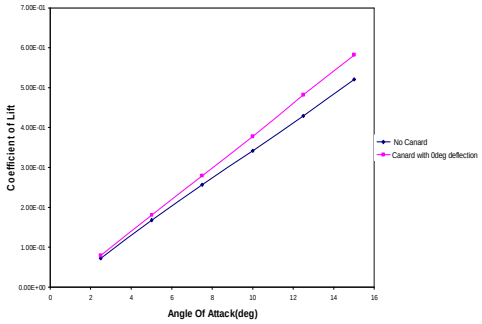

Fig 3.41 Comparison of C_L between δ_c = 0deg and No canard configuration

CONCLUSION

The present study shows the effect of Canard-Wing-Body combination for a generic modern fighter type of aircraft configuration. A CFD simulation has been used in the present analysis. The flow features are obtained using CFD package HYENA. The effect of canard control surface is studied and was subjected to various canard deflection angles.

Geometric modeling was carried out using Catiav5, the details are as follows:Scaling of the prototype aircraft prior to smoothening

Smoothening the individual parts of candidate fighter aircraft.

Assembling the intake to the candidate fighter aircraft.Deflection of the canard to +10deg angle.Deflection of the canard to -10deg angle. The generation of grid was carried out using ANYSY ICEMCFD. The computational domain and the cells of the reference mesh were of tetrahedral type.

Finite volume analysis was carried out to predict the aerodynamic characteristics namely, coefficient of lift, coefficient of drag, and coefficient of pitching moment using HYENA and the results are presented in tables 8.1 to 8.4 and in figures 8.8 to 8.10, 8.18 to 8.20, 8.28 to 8.30, and 8.38 to 8.46.

The flow visualization of streamline traces for the following cases namely, .canard control deflections of 0, -10 & 10 degrees and for the angle of attack of 0, 2.5, 5, 7.5, 10, 12.5 and 15 degrees at a free stream Mach number 0.5 have been computed and were presented in figures 8.2 to 8.7, 8.12 to 8.17, 8.22 to 8.27, and 8.32 to 8.37.

It is observed from the computed CFD results for the case of canard deflection of 10^0 at angle of attack of 15^0, the L/D ratio improvement is about 9%.Referring to figure 8.20 and 8.30 it is observed that for the canard control deflection of 10^0 and angle of attack of 15^0, pitch control effectiveness is significantly increased. From the above analysis, it may be evident that the aircraft with canard configuration is more effective than an aircraft configuration without canard.

REFERENCES

1. Kuchemann, "Boundary Layer Characteristics of the Miley Airfoil at Low Reynolds Numbers," J. Aircr, vol. 21, no. 9, pp. 658-664, September 1984.

2. Grosche, "The Application of Computational Fluid Dynamics to Aircraft Design," AIAA paper 86-2651, 1986.

3. Loeve, "Numerical Solutions of the Euler Equations by Finite Volume Methods Using Runge-Kutta Time Stepping Schemes," AIAA paper 81-1259, 1981.

4. Lock , “Numerical Computation of Internal and External Flows”, vol. I:

Fundamentals of Numerical Discretization, Wiley, New York, 1988

5. Carmichael, "Computational Aerodynamics Development and Outlook," AIAA J., vol. 17, no. 12, pp. 1293-1313, December 1979.

6. Gregoriou, "Numerical Investigation of the Laminar, Supersonic Flow over a Rearward- Facing Step Using an Adaptive Grid Scheme" M.S. thesis, Department of Aerospace Engineering, University of Maryland, College Park, 1982.

7. Shrout, "Applied Computational Aerodynamics, Progress in Astro-Astronautics and Aeronautics Series", vol. 125, AIAA, Washington, D.C., chap. 4, pp. 91-130, 1990.

8. Liu, Da-Ming, Computational Techniques for Fluid Dynamics, vol. II: Specific Techniques for Different Flow Categories, Springer-Verlag, Berlin, 1988.

9. Ottensoser,Jonah, Computational Fluid Dynamics for Engineers, Engineering Education System, Austin, Tex., 1989.

10. Paulson, J. W., Jr.; Thomas, J. L, Transitions and interactions of inviscid/viscous, compressible/incompressible, and laminar/turbulent flows. Int. J. Num. Meth.Fl,31,223^6.

11. Paulson, J. W., Jr.; Thomas, J. L.; Winston, M. M, "Adaptive Solutions for Compressible Flows on Unstructured, Strongly Anisotropic Grids," in C. Hirsch, J. Periaux, and W. Kordulla (eds.), Computational Fluid Dynamics '92, vol. 2, Elsevier, Amsterdam, 1992, pp. 945-951.

12. Thomas, J. L.; Paulson, J. W., Jr.; Yip, L. P, "Comparative Study of Inviscid and Viscous Flows Over an STS," Computational Fluid Dynamics '92, vol. 1, Elsevier, Amsterdam, 1992, pp. 323-330.

13. Joseph P. Landfield* and Dario Rajkovict, "Multigrid for Hypersonic Viscous Two- and Three-Dimensional Flows," AIAA paper 91-1572-CP, Proc. AIAA 10thComput. Fluid Dyn. Conf, 1991.

14. ICEM-CFD Tutorial Manual: Meshing Modules Version 11, ANSYS, Inc.

15. ADA Internal report

16. Catia v5 help